Current-mode Biquadratic Universal Filter Design with Two Terminal Unity Gain Cells

Halil ALPASLAN, Erkan YUCE

Dept. of Electrical and Electronics Engineering, Pamukkale University, Kinikli, 20070 Denizli, Turkey

alpaslanster@gmail.com, erkanyuce@yahoo.com

Abstract. *A grounded parallel lossy active inductor and two current-mode (CM) universal filters are presented in this paper. All the circuits use two voltage followers (VFs) and a current follower (CF). The parallel lossy active inductor includes a grounded capacitor which is attractive in integrated circuit (IC) technology. The CM universal filters have one input and standard three outputs such as band-pass (BP), low-pass (LP) and high-pass (HP) responses. All-pass and notch outputs can be obtained by adding extra one CF. Suggested structures in this paper can be constructed with commercially available active devices such as AD844s. Non-ideal gain and intrinsic X-terminal parasitic resistor effects are examined. Several computer simulations with SPICE program and experimental results by employing AD844s are drawn to verify theoretical ones.*

Keywords.

Lossy inductor simulator, current-mode filter, unity gain cell, current follower, voltage follower.

1. Introduction

Active filters can be easily realized in integrated circuits (ICs) instead of standard passive filters. Therefore, they have been used in many analog applications from past to present [1-3]. Besides, they can be classification such as current-mode (CM) filters and voltage-mode (VM) filters. CM signal processing cause higher frequency of operation due to small load resistor and wide dynamic range of CM active devices [4]. Second generation current conveyors (CCIIs) are well known active devices [5]. Non-ideal voltage and current gains restrain the CCII performances. Current followers (CFs) and voltage followers (VFs) known as unity gain cells (UGCs) have quite small active sensitivities [6], [7]. UGCs are widely used for avoiding double non-ideal current and voltage gain effects of the CCIIs in designing active filters in the open literature [6-12].

CM biquadratic universal filter in [6] uses two CFs, one of which is plus type while the other one is minus type, one VF and four admittances. Furthermore, the LP output is obtained from resistor between VF and minus type CF. CM universal biquad in [7] uses a CF and a VF and five admittances. CM filter of [7] has a band-pass gain which is less than unity. Proposed CM biquadratic filter in [8] uses six UGCs, three of which are used as CFs whereas the others are employed as VFs, and nine admittances. One of the CM universal filters in [9] uses four CFs, three VFs and eight admittances for three inputs and one output current. Other circuit in [9] contains three CFs and three VFs and eight passive components for one input three output currents. CM filter in [10] is composed of three CFs, two VFs and six admittances where used technology is 1.2μm CMOS process. Moreover, the used CFs have two outputs. In [11], two universal CM filters, designed by BJT technology, one of which is multi input multi output filter which has three dual output CFs, one VF and four passive components. The other one is multi input single output filter which has one dual output CF, one single output CF, one VF and four passive components. Proposed filter circuit in [12] which is VM/ CM includes four VFs, four dual output CFs and seven passive components in which power supply voltages are ±5 V and used technology is 1.2μm CMOS process. Also, it has a complex internal structure. The universal filter in [13] need to revise of some element connections and/or used elements. In [14], the proposed first and third filter configurations use nano-Farads level capacitors. The other current-mode filter circuit in [15] is one input one output based on current mirror arrays. Besides, its power supply voltages are ±5 V and used technology is 0.8μm CMOS process. In [16], the proposed modified CM universal filter has more active components which are four digitally controlled CF, two dual-output CF, two buffers. On the other hand, the universal filters can be used in some applications for example, intermediate frequency stages of transmitters and receivers, some telephone decoder and crossover networks [17].

In this study, two second-order universal filters which are derived from an electronically tunable lossy grounded inductor simulator are composed of two VFs and one CF and a smaller number of passive components. The suggested parallel grounded lossy inductor includes a grounded capacitor, which is advantageous in IC technology [18, 19]. The first filter can provide gains for low-pass and band-pass responses while the second (reorganized) one can realize a gain for only low-pass response. The developed filters from the parallel grounded lossy inductor can simultaneously provide all the standard filter responses such as low-pass (LP), band-pass (BP) and high-pass (HP) responses. Also, notch and all-pass responses can be easily obtained by adding an extra CF to the introduced filters. All proposed circuits can be constructed with commercially available active devices such as AD844s [20]. Some simulation and experimental results are included to confirm the theory.

Content of this study is organized as follows: after description of the UGCs in section two, identification of the proposed universal filters in section three is given. Designation of the simulation and experimental results are respectively given in sections four and five. Conclusion is given in the last section, section six.

2. Unity Gain Cells

A CF+ can be obtained from a CCII+ by grounding y-terminal of the CCII+ and a VF can be obtained from a CCII+ by grounding z-terminal of the CCII+ [5]. Electrical symbols of the CF+ and VF are shown in Fig. 1. The CF+ and VF are ideally defined in (1) and (2), respectively.

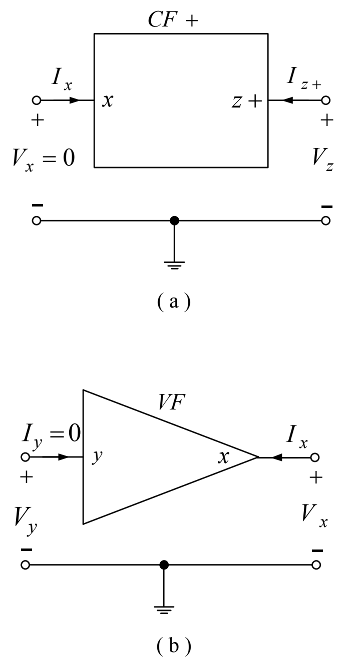

Fig. 1. Symbolic representation of (a) CF+, (b) VF.

$$V_x = 0,\ I_z = I_x, \tag{1}$$

$$I_y = 0,\ V_x = V_y. \tag{2}$$

Including non-ideal current gain of the CF+ and non-ideal voltage gain of the VF together with their parasitic impedance effects, the CF+ and VF can be characterized in (3) and (4), respectively.

$$\begin{bmatrix} I_z \\ V_x \end{bmatrix} = \begin{bmatrix} sC_z + \dfrac{1}{R_z} & \alpha(s) \\ 0 & Z_x(s) \end{bmatrix} \begin{bmatrix} V_z \\ I_x \end{bmatrix}, \tag{3}$$

$$\begin{bmatrix} I_y \\ Vx \end{bmatrix} = \begin{bmatrix} sCy + \dfrac{1}{Ry} & 0 \\ \beta(s) & Z_x(s) \end{bmatrix} \begin{bmatrix} Vy \\ Ix \end{bmatrix}. \tag{4}$$

Frequency dependent non-ideal current gain of the CF+ is $\alpha(s) = \alpha_0 / (1+s/w_\alpha)$ as well as frequency dependent non-ideal voltage gain of the VF is $\beta(s) = \beta_0 / (1+s/w_\beta)$. The DC non-ideal gains are $\alpha_0 = 1 + \varepsilon_\alpha$ and $\beta_0 = 1 + \varepsilon_\beta$ which are ideally equal to unity. Their bandwidths, w_α and w_β, are ideally equal to infinity. In addition to this knowledge, $-1 << \varepsilon_\alpha << 1$ and $-1 << \varepsilon_\beta << 1$ are known as current tracking error and voltage tracking error, respectively. Fortunately, the pole frequencies f_α and f_β are effective at high frequencies; therefore, their effects can be ignored at low and medium frequencies. However, CFs have no voltage gain effects because of the virtual ground at their input terminals and also VFs have no current gain effects. Parasitic resistors R_z and R_y and parasitic capacitances C_z and C_y are the parasitics of z and y terminals of the CF+ and VF, respectively. The X-terminal has a parasitic impedance $Z_x(s) = (1/sC_x)\ //\ (R_x + sL_x)$ which is ideally equal to zero. In this study, the CMOS CCII structure of [21] in Fig. 2 is used for the CF+ and VF.

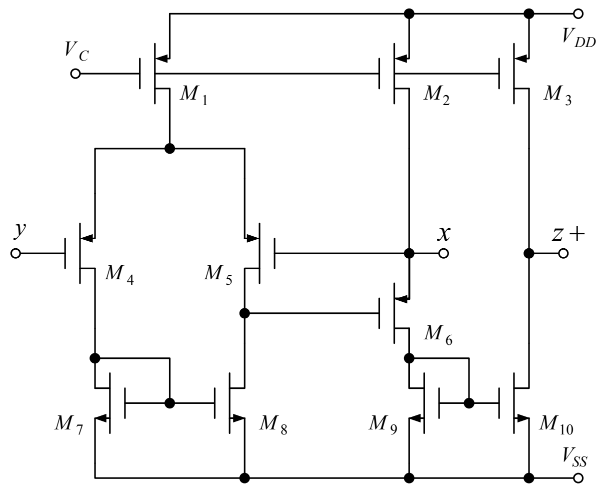

Fig. 2. CMOS CCII internal structure of [16].

3. Proposed Universal Filters

A simple passive filter can be obtained by using parallel R-L-C and/or series R-L-C circuits. In addition, an active inductor circuit can be used instead of passive inductor in a filter circuit. As a result, an active filter can be constituted by making some modifications such as adding some passive circuit elements on active inductor circuits [22], [23]. A grounded active inductor topology and its equivalent circuit are given in Fig. 3 and 4, respectively.

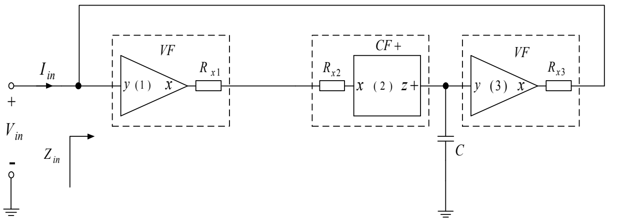

Fig. 3. Proposed active inductor circuit.

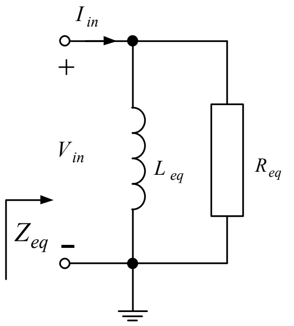

Fig. 4. Symbolic equivalent circuit of the proposed inductor.

Input impedance equation of the proposed inductor is given in (5).

$$Z_{eq}(s)=\frac{1}{\dfrac{1}{R_{eq}}+\dfrac{1}{sL_{eq}}}$$
$$Z_{in}(s)=\frac{1}{\dfrac{1}{R_{x3}}+\dfrac{\beta_1\alpha_2\beta_3}{sC(R_{x1}+R_{x2})R_{x3}}} \tag{5}$$

Equivalent resistance is equal to R_{x3} and equivalent inductance is equal to $C(R_{x1}+R_{x2})R_{x3}$ / $\beta_1\alpha_2\beta_3$, which can be seen from (5).

Characteristic equations ($D_1(s)$ with only parasitic resistors and $D_2(s)$ with only non-ideal gains) of the filter transfer functions (TFs) in Fig. 5 are given in (6), where $R_a = R_2 + R_{x2}$. Besides, X-terminal parasitic resistors of the UGCs (R_{x1}, R_{x2} and R_{x3}) and non-ideal gains affect the filter TFs as seen from (7) and (8), respectively.

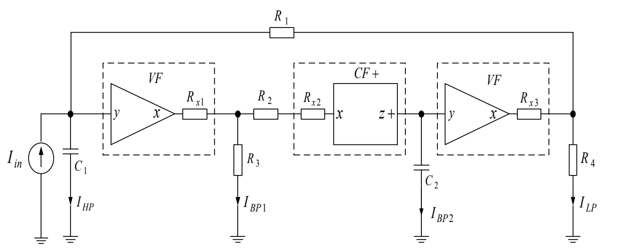

Fig. 5. The first proposed biquadratic universal filter.

$$D_1(s)=a_2s^2+a_1s+a_0 \tag{6.a}$$

Here,

$$a_2=C_1C_2(R_1R_4(R_aR_{x1}+R_3(R_a+R_{x1}))+$$
$$+(R_1+R_4)(R_aR_{x1}+R_3(R_a+R_{x1}))R_{x3})$$
$$a_1=C_2(R_4R_aR_{x1}+R_3R_4(R_a+R_{x1})+$$
$$+(R_aR_{x1}+R_3(R_a+R_{x1}))R_{x3})$$
$$a_0=R_3+R_4$$

$$D_2(s)=s^2C_1C_2R_1R_2+sC_2R_2+\alpha_2\beta_2\beta_3 \tag{6.b}$$

$$\frac{I_{HP}}{I_{in}}=\frac{s^2C_1C_2(R_aR_{x1}+R_3(R_a+R_{x1}))(R_4R_{x3}+R_1(R_4+R_{x3}))}{D_1(s)} \tag{7.a}$$

$$\frac{I_{BP1}}{I_{in}}=\frac{sC_2R_a(R_4R_{x3}+R_1(R_4+R_{x3}))}{D_1(s)} \tag{7.b}$$

$$\frac{I_{BP2}}{I_{in}}=-\frac{sC_2R_3(R_4R_{x3}+R_1(R_4+R_{x3}))}{D_1(s)} \tag{7.c}$$

$$\frac{I_{LP}}{I_{in}}=\frac{sC_2R_{x3}(R_aR_{x1}+R_3(R_a+R_{x1})-R_1R_3R_{x3}}{D_1(s)} \tag{7.d}$$

$$\frac{I_{HP}}{I_{in}}=\frac{s^2C_1C_2R_1R_2}{D_2(s)} \tag{8.a}$$

$$\frac{I_{BP1}}{I_{in}}=\frac{R_1}{R_3}\frac{sC_2R_2\beta_1}{D_2(s)} \tag{8.b}$$

$$\frac{I_{BP2}}{I_{in}}=-\frac{sC_2R_1\beta_1\alpha_2}{D_2(s)} \tag{8.c}$$

$$\frac{I_{LP}}{I_{in}}=-\frac{R_1}{R_4}\frac{\beta_1\alpha_2\beta_3}{D_2(s)} \tag{8.d}$$

When included both non-ideal gains and parasitic resistors, equations for the filter TFs are much more complex. Thus, the proposed universal filter circuit is reorganized as seen from Fig. 6, the second suggested filter.

Characteristic equation, $D_3(s)$, for the filter in Fig. 6 is given in (9) where $R_b = R_{x1} + R_{x2} + R_2$. Current TFs, angular resonance frequency (w_0) and quality factor (Q) including non-ideal gain and parasitic resistor effects for the reorganized second-order universal filter circuit are given in (10) and (11).

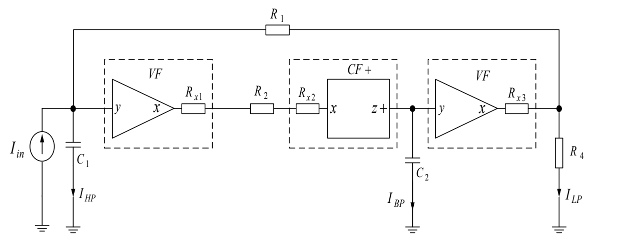

Fig. 6. The second proposed second-order universal filter.

$$D_3(s)=s^2C_1C_2R_b(R_1R_4+R_1R_{x3}+R_4R_{x3})+$$
$$+sC_2R_b(R_4+R_{x3})+R_4\beta_1\alpha_2\beta_3 \tag{9}$$

$$\frac{I_{HP}}{I_{in}}=\frac{s^2C_1C_2R_b(R_1R_4+R_1R_{x3}+R_4R_{x3})}{D_3(s)} \tag{10.a}$$

$$\frac{I_{BP}}{I_{in}}=-\frac{sC_2(R_1R_4+R_1R_{x3}+R_4R_{x3})\alpha_2\beta_1}{D_3(s)} \tag{10.b}$$

$$\frac{I_{LP}}{I_{in}}=\frac{sC_2R_bR_{x3}-R_1\beta_1\alpha_2\beta_3}{D_3(s)} \tag{10.c}$$

$$w_0 = \sqrt{\frac{R_4\beta_1\alpha_2\beta_3}{C_1C_2R_b(R_1R_4 + R_1R_{x3} + R_4R_{x3})}} \qquad (11.a)$$

$$Q = \frac{1}{R_4 + R_{x3}}\sqrt{\frac{C_1(R_1R_4 + R_1R_{x3} + R_4R_{x3})R_4\beta_1\alpha_2\beta_3}{C_2R_b}} \qquad (11.b)$$

Ideal form equations for the two universal filters are given from (12) to (14).

$$D(s) = s^2C_1C_2R_1R_2 + sC_2R_2 + 1 \qquad (12)$$

$$\frac{I_{HP}}{I_{in}} = \frac{s^2C_1C_2R_1R_2}{D(s)} \qquad (13.a)$$

$$\frac{I_{BP1}}{I_{in}} = \frac{R_1}{R_3}\frac{sC_2R_2}{D(s)} \qquad (13.b)$$

$$\frac{I_{BP2}}{I_{in}} = \frac{I_{BP}}{I_{in}} = -\frac{sC_2R_1}{D(s)} \qquad (13.c)$$

$$\frac{I_{LP}}{I_{in}} = -\frac{R_1}{R_4}\frac{1}{D(s)} \qquad (13.d)$$

$$w_0 = \frac{1}{\sqrt{C_1C_2R_1R_2}} \qquad (14.a)$$

$$Q = \sqrt{\frac{C_1R_1}{C_2R_2}} \qquad (14.b)$$

Sensitivity analysis is accomplished in order to examine the performance of the proposed universal filters. Passive sensitivity values of the proposed filter with respect to w_0 and Q for the ideal equations in (14) are found in (15).

$$S^{w0}_{R_1,R_2,C_1,C_2} = S^{Q}_{R_2,C_2} = -S^{Q}_{R_1,C_1} = -\frac{1}{2} \qquad (15)$$

If previous stage of the proposed filters is not high output impedance, extra one CF is used for each of the filters. Similarly, if the next stage of the proposed filters is not low input impedance, extra one CF is used for each response. In addition to these, if one of the capacitor of the proposed filters is removed from ground and connected to the X terminal of the additional CF to obtain high output impedance current, the high frequency of the proposed filters can be affected [24]. Therefore, the parasitic resistor of the X terminal of the additional CF should be chosen as small as possible to improve high frequency performance of the suggested filter.

4. Simulation Results

All the simulations are performed by means of SPICE in which symmetrical power supply voltages are selected as $V_{DD} = -V_{SS} = 1.25$ V and $V_c = 0.4$ V is chosen. The proposed grounded parallel lossy inductor with passive element $C = 10$ pF and $R_{x1} = R_{x2} = R_{x3} = 63.66\ \Omega$ yielding $L_{eq} = 81.02$ nH and $R_{eq} = 63.66\ \Omega$ are simulated, the results are shown in Fig. 7. The first proposed filter and its reorganized form have $R_1 = R_4 = 2$ kΩ, $R_2 = 1.2$ kΩ, ($R_3 = 2$ kΩ which is used only for the first filter), $C_1 = 100$ pF and $C_2 = 10$ pF. This passive component values result in $Q \approx 4.08$ and $f_o \approx 3.248$ MHz. The CMOS CCII structure given in Fig. 2 is sized with standard 0.25μm technology. All the MOS transistors are worked in saturation region for all simulations. Also, aspect ratios of the MOS transistors are given in Tab. 1.

MOS transistors	W(µm)	L(µm)
M_1, M_4, M_5	20	0.5
M_2, M_3	40	0.5
M_6	80	0.5
M_7, M_8, M_9, M_{10}	12	0.5

Tab. 1. Dimensions of the used CMOS transistors in Fig. 2.

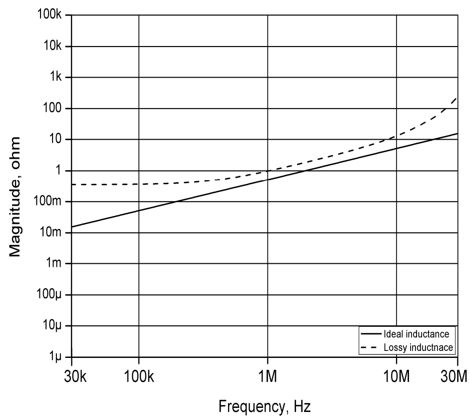

Fig. 7. AC analysis results for the lossy inductor.

3dB cutoff frequency of I_{C1} is restricted by the X-terminal resistors. However, when the resistor R_3 is used, this restriction can be more effective, which is shown in Fig. 8.

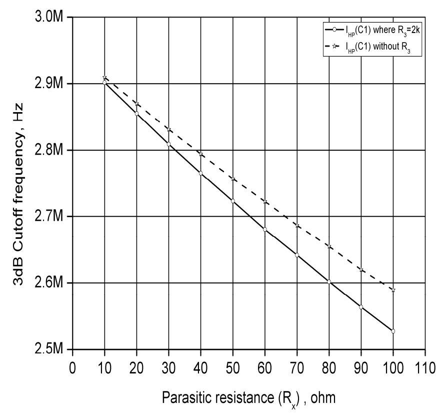

Fig. 8. Effects of the resistor R_3 on the proposed CM universal filters.

In this study, MC analysis for a hundred simulation runs is made by applying 10% deviation on capacitor C_2 for the first and second developed universal filters. Simulation results related with MC analysis are given in Fig. 9 and 10, respectively. As seen from the MC analysis, the capacitor C_2 and resistor R_3 affect the filter performance. Moreover, both capacitor C_1 and resistor R_3 effects on the proposed filter are given in Fig. 11.

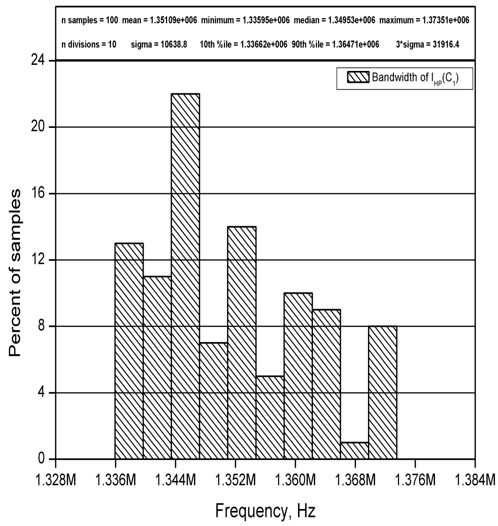

Fig. 9. MC analysis for the first proposed filter.

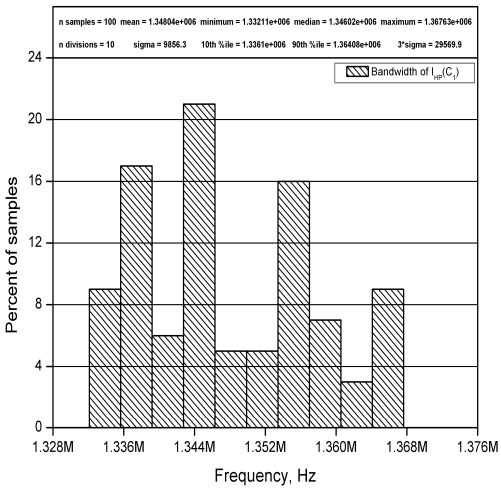

Fig. 10. MC analysis for the second proposed filter.

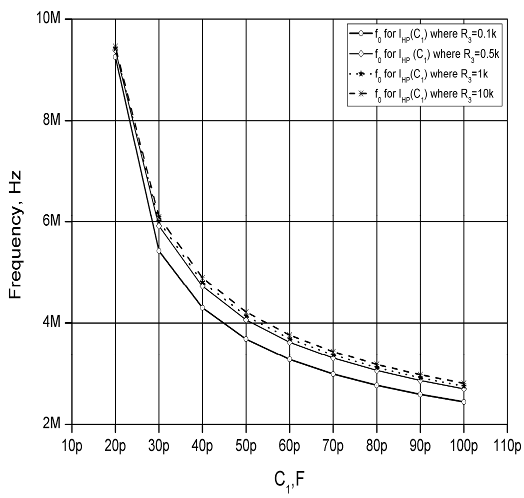

Fig. 11. Impact on the 3dB cutoff frequency of I_{C1} by changing C_1 and R_3.

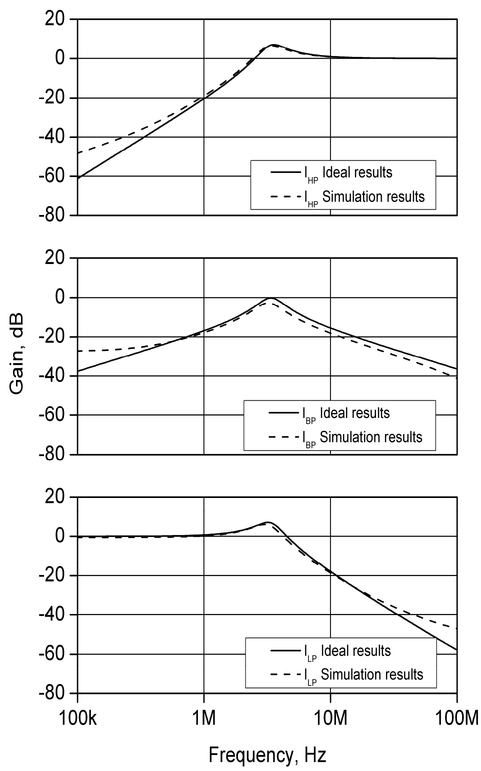

Fig. 12. The first proposed filter TFs in AC analysis.

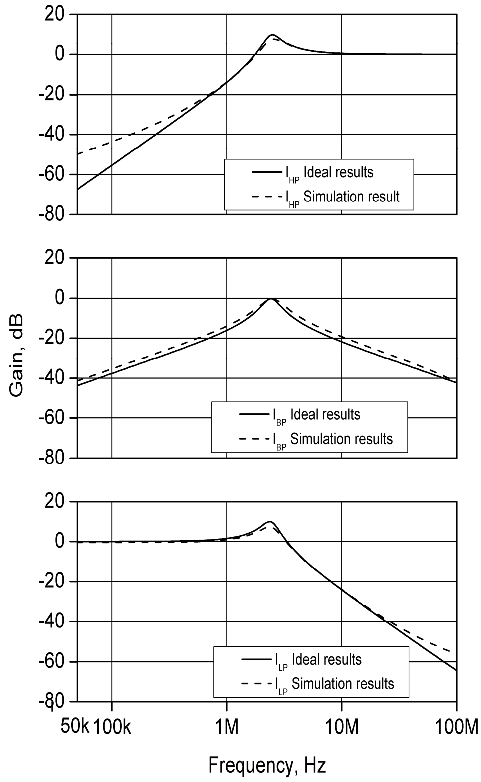

Fig. 13. AC analysis results for the reorganized filter.

AC analysis of the first proposed universal filter outputs such as BP, HP and LP responses is given in Fig. 12. AC analysis of the reorganized universal filter TFs such as BP, HP and LP responses is given in Fig. 13.

While C_2 is changing from 10 pF to 100 pF with 30 pF steps and input current magnitude is 50 μA, step response of the HP output current on C_1 and BP output current on C_2 for the reorganized universal filter are given in Fig. 14. Q and step response are interrelated as seen from Fig. 14. In theory, impending ζ is damping factor and σ is attenuation. Q, according to these parameters, is given in (16) [25]. The unit step signal with 50 μA current amplitude and 0.1 μs rise time is applied to the proposed filter. Moreover, the result of the filter current outputs on C_1 and C_2 are given in Fig. 14.

$$Q = \frac{1}{2\zeta} = \frac{w_0}{2\sigma} \tag{16}$$

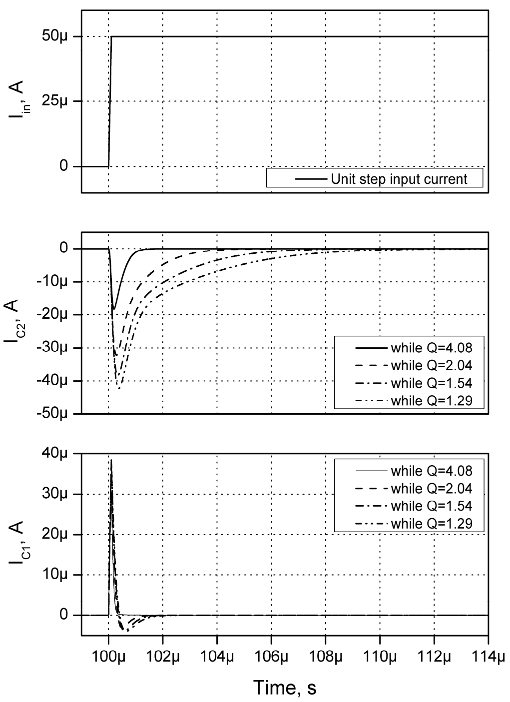

Fig. 14. The responses to the input unit step signal of the second universal filter.

Total harmonic distortion (THD) results for HP and BP TFs of the reorganized filter circuit are shown in Fig. 15.

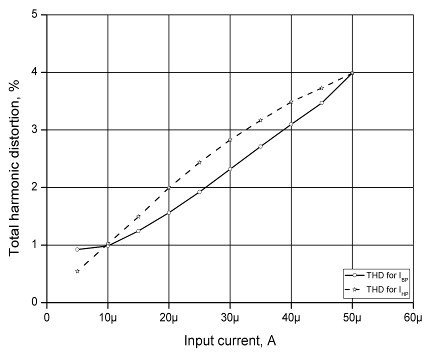

Fig. 15. THD results as changing input current magnitude.

Fast Fourier transform (FFT) simulation for the second filter circuit is made where 25 μA and 50 μA input sinusoidal signals are separately applied and results are given in Fig. 16. Besides, noise effects for the second filter circuit are given in Fig. 17. For the second filter, the NOISE values are quite small and THD value is under 4% even input current magnitude is 50 μA. Besides, total power dissipation for the second filter circuit is evaluated as 6.87 mW.

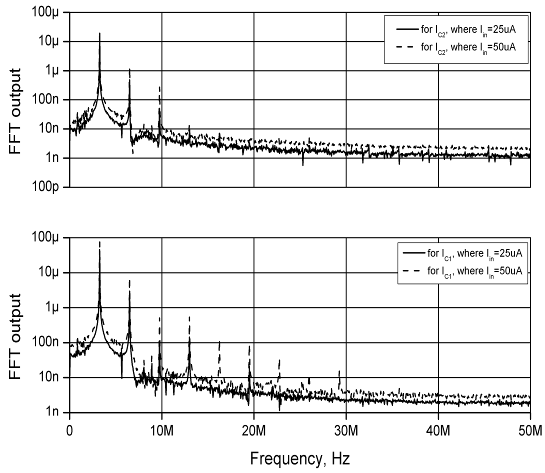

Fig. 16. FFT simulation results.

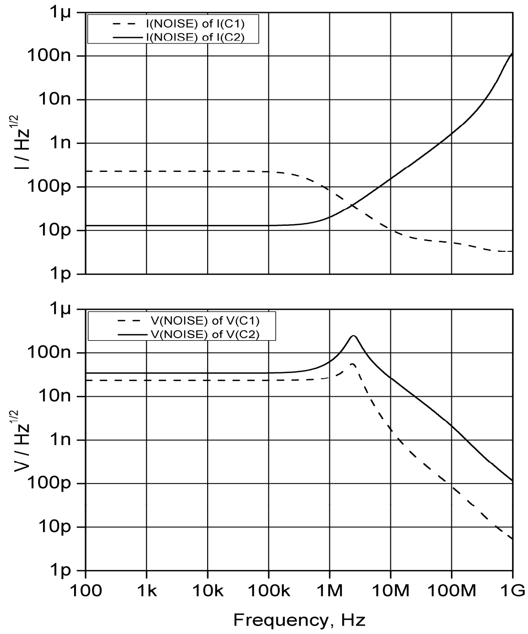

Fig. 17. NOISE simulation results.

5. Experimental Results

Tests are made on the first proposed CM universal filter. The commercially available active structures, AD844s, with BJTs and known as 60MHz 200V/µs monolithic op amp IC are used in the test circuit where one of the AD844s is used to obtain current source.

Passive components are chosen as $R = 300\ \Omega$, $R_1 = R_3 = R_4 = 1\ \text{k}\Omega$, $R_2 = 100\ \Omega$, $C_1 = C_2 = 100$ pF and power supply voltages are adjusted to $V_{DD} = -V_{SS} = 12$ V. Three AD844 ICs are used in test circuit given in Fig. 18. For this test circuit, $Q \approx 3.162$ and $f_0 \approx 5.03$ MHz are calculated. Besides, both ideal and experimental results are given in Fig. 19.

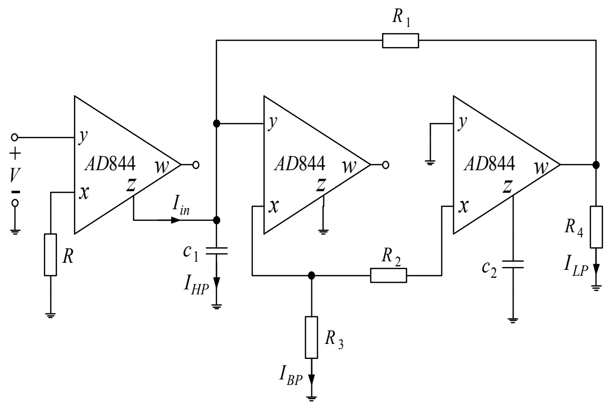

Fig. 18. Test circuit designed with AD844 ICs.

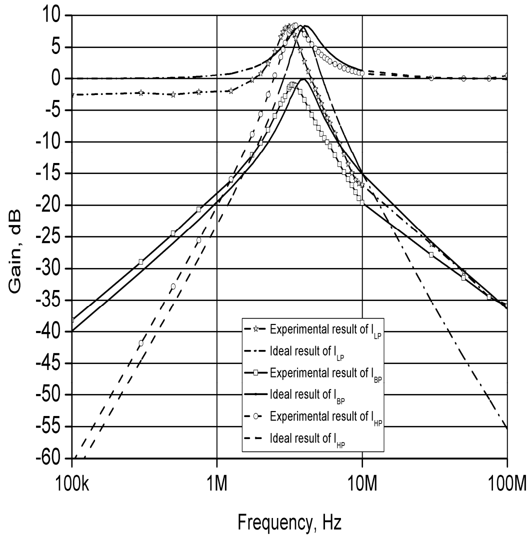

Fig. 19. Experimental results of the first suggested CM second-order universal filter.

6. Conclusion

In this work, we present a grounded parallel lossy active inductor simulator and two versions of single input multi output CM universal filters for simultaneously providing HP, LP, BP outputs. All the introduced configurations in this paper consist of two VFs and a CF. The suggested parallel grounded lossy inductor includes a grounded capacitor, which is advantageous in IC fabrication. By adding an extra CF to the filter circuits, all-pass and notch filter output currents can be easily obtained. In addition to these, all the topologies can easily be constructed by employing commercially available active devices such as AD844s. Non-ideal gain and X-terminal parasitic resistor effects are examined in this paper. The claimed theory, simulation results and experimental results are compatible with themselves.

References

[1] MARISCOTTI, A. An active analog filter architecture ensuring unity-gain and low sensitivity. *Circuit Syst. Signal Process*, 2010, vol. 29, p. 745-756, 2010.

[2] SUN, Y. Design of high frequency integrated analogue filters. The Institution of Engineering Tech., April 15, 2002.

[3] GHAUSI, M. S. Analog active filters. *IEEE Trans. on Circuits and Systems*, 1984, vol. 31, p. 13-31.

[4] RAUT, R., SWAMY, M. N. S. *Modern Analog Filter Analysis and Design: A Practical Approach*. Wiley-VCH, 1st edition, 2010.

[5] FERI, G., GUERRINI, N. C. *Low Voltage, Low Power CMOS Current Conveyor*. Springer, 1st edition, 2003.

[6] WENG, R.-M., LEE, M.-H. Novel universal biquad filters using only three followers. *Int. Journal of Electronics*, 1997, vol. 82, p. 621-628.

[7] WENG, R.-M., LEE, M.-H. Novel universal biquad filters using only two unity-gain cells. *Int. Journal of Electronics*, 2000, vol. 87, p. 57-61.

[8] CELMA, S., SABADELL, J., MARTINEZ, P. Universal filter using unity-gain cells. *Electronic Letters*, 1995, vol. 31, p. 1817 to 1818.

[9] ABUELMA'ATTI, M. T., AL-QUAHTANI, M. A. Current-mode universal filters using unity-gain cells. *Electronic Letters*, 1996, vol. 32, p. 1077-1079.

[10] ALZAHER, H. A., ISMAIL, M. Current-mode universal filter using unity-gain cells. *Electronic Letters*, 1999, vol. 35, p. 2198 to 2200.

[11] CHANG, C.-M., LIAO, T.-S., YU, T.-Y., LIN, E.-S., TENG, C.-H., HOU, C.-L. Novel universal current-mode filters using unity-gain cells. *Int. Journal of Electronics,* 2001, vol. 88, p. 23-30.

[12] GUPTA, S. S., SENANI, R. New voltage-mode/current-mode universal biquad filter using unity-gain cells. *Int. Journal of Electronics,* 2006, vol. 93, p. 769-775.

[13] SENANI, R., GUPTA, S. S. Universal voltage-mode/current-mode biquad filter realised with current feedback op-amps. *Frequenz*, 1997, vol. 51, p. 203-208.

[14] LIU, S.-I., CHEN, J.-J., HWANG, Y.-S. New current mode biquad filters using current followers. *IEEE Trans. on Circuits and Systems –I: Fund. Theory and Applications,* 1995, vol. 42, p. 380 to 383.

[15] SOULIOTIS, G., HARITANTIS, I. Current-mode filters based on current mirror arrays. *Int. J. Circ. Theor. Appl.*, 2007, vol. 36, p. 173-183.

[16] ALZAHER, H. A. A CMOS digitally programmable universal current-mode filter. *IEEE Trans. on Circuits and Systems –II: Express Briefs,* 2008, vol. 55, p. 758-762.

[17] PAARMANN, L. D. *Design and Analysis of Analog Filters: A Signal Processing Perspective*. Kluwer Academic Publisher, 2001.

[18] YUCE, E. Fully integrable mixed-mode universal biquad with specific application of the CFOA. *International Journal of Electronics and Communications (AEU)*, 2010, vol. 64, no. 4, p. 304-309.

[19] YUCE, E. A novel floating simulation topology composed of only grounded passive components. *International Journal of Electronics*, 2010, vol. 97, no. 3, p. 249-262.

[20] AD844 monolithic op amp. [Online] Available at: http: //www.analog.com/static/imported-files/data_sheets/AD844.pdf

[21] SURAKAMPONTORN, W., RIEWRUJA, V., KUMWACHARA, K., DEJHAN, K. Accurate CMOS-based current conveyors. *IEEE Transactions on Instrumentation and Measurement*, 1991, vol. 40, p. 699-702.

[22] FABRE, A., SAAID, O., WIEST, F., BOUCHERON, C. Current controlled bandpass filter based on translinear conveyors. *Electronic Letters*, 1995, vol. 31, p. 1727-1728.

[23] FABRE, A., SAAID, O., WIEST, F., BOUCHERON, C. Low power current-mode second-order bandpass IF filter. *IEEE Transactions on Circuits and Systems-II: Analog and Digital Signal Processing*, 1997, vol. 44, p. 436-446.

[24] YUCE, E., MINAEI, S. Universal current-mode filters and parasitic impedance effects on the filter performances. *International Journal of Circuit Theory and Applications,* 2008, vol. 36, p. 161-171.

[25] OGATA, K. *Modern Control Engineering.* Prentice Hall, 4th edition, 2001.

About Authors

Halil ALPASLAN received the B.Sc. and the M.Sc. degrees from Pamukkale University, Department of Electrical and Electronics Engineering in Denizli, Turkey in 2001 and 2005, respectively. He is currently a PhD student at Pamukkale University, Institute of Science and Technology, Department of Electrical and Electronics Engineering in Denizli, Turkey. He has been working as a research assistant at Pamukkale University since 2001. His research interests include analog current mode circuits, analog integrated circuit design, unity gain cells and current conveyors.

Erkan YUCE was born in 1969 in Nigde, Turkey. He received the B.Sc. degree from Middle East Technical University, the M.Sc. degree from Pamukkale University and the PhD. degree from Bogazici University, all in Electrical and Electronics Engineering in 1994, 1998 and 2006, respectively. He is currently an Associative Professor at the Electrical and Electronics Engineering Department of Pamukkale University. His current research interests include analog circuits, active filters, synthetic inductors and CMOS based circuits. He is the author or co-author of about 90 papers published in scientific journals or conference proceedings.